Simulation and experimental characterization of SOA-MZI-based multiwavelength conversion

Simulation and Experimental Characterization of SOA-MZI-Based Multiwavelength Conversion

N. Yan, *Student Member, IEEE*, J. del Val Puente, T. G. Silveira, *Student Member, IEEE*, A. Teixeira, *Member, IEEE*, A. P. S. Ferreira, *Student Member, IEEE*, E. Tangdiongga, P. Monteiro, *Member, IEEE*, and A. M. J. Koonen, *Fellow, IEEE*

***Abstract*—We present, for the first time, extensive simulation and experimental characterizations of single SOA-MZI-based multiwavelength conversion (MWC) of NRZ data at 10 Gb/s and RZ data at 40 Gb/s under various parametric conditions deploying ITU standard 100- and 200-GHz channel spacing. We analyze, in particular, the physical performance impairments caused by high-order four-wave mixing interference. Our simulation results indicate the promising performance of the MWC up to eight channels with 200-GHz channel spacing. We further experimentally demonstrate four-channel 10-Gb/s error-free MWC with signal regeneration possibilities and 40-Gb/s MWC with moderate penalties, based on commercially available integrated SOA-MZIs. We obtained clear, open converted eye diagrams and achieved negligible difference in channel performance among all MWC channels at both bit rates. Our results proved the excellent performance of a simple scheme for various future network and system applications, such as all-optical wavelength multicast and grid networking.**

***Index Terms*—All-optical, cross-phase modulation (XPM), multicast, multiwavelength conversion (MWC), semiconductor optical amplifier-Mach–Zehnder interferometer (SOA-MZI), wavelength division multiplexing (WDM).**

I. Introduction

OPTICAL wavelength division multiplexing (WDM) systems have been deployed in data transmission links over the last decade to meet the rapidly increasing bandwidth demand [1]. The exponential growth of Internet and multimedia traffic poses a potential challenge for the telecommunication transport networks. Emerging voice-over-Internet protocol, video streaming, high-definition TV, and peer-to-peer file transfer services are becoming widely available on top of the traditional Internet services. In order to deliver large amount of data efficiently, more and more networking functions that are currently performed by electronics are to be moved to the optical layer. Telecommunication networks are undergoing major transformations driven by new all-optical technologies for WDM applications. All-optical solutions for switching, routing and multicasting become of crucial importance for realizing a truly intelligent, transparent, and broadband optical infrastructure.

All-optical wavelength conversion (AOWC) is a key WDM functionality for network interoperability and scalability. It can be used to route and switch wavelengths, resolve contention, reduce node blocking probabilities, increase optical transparency, and enable dynamic network wavelength assignments and allocation capability [1], [2]. As AOWC technologies are walking into a mature stage of high bit rates at 10–40 Gb/s and successful research demonstration at 160–320 Gb/s [3] crossing the last two decades, all-optical multiwavelength conversion (MWC) began to attract increasing interest during the last five years due to several advantages. First, instead of deploying large amount of optical-electronic-optical (OEO) transponders and electronics, all-optical MWC can be realized in a single device such as a semiconductor optical amplifier (SOA) Mach–Zehnder interferometer (MZI), saving operational cost and reducing system complexity. Second, it provides more independency on bit rate, protocol, modulation format and utilized bandwidth. Unlike with OEO MWC, physical resources for all-optical MWC do not need to be replaced, upgraded or multiplied whenever a change takes place concerning the above mentioned system parameters. Finally, all-optical MWC has also facilitated many new applications, such as optical layer wavelength multicast [4]–[7], grid networking [8], and service multi- or broadcast in access networks [4].

Various all-optical MWC techniques have been demonstrated in recent years. Promising results have been shown based on technologies in the following categories: four-wave mixing (FWM) [7], [9] or supercontinuum [10], cross-phase modulation (XPM) [4], [11]–[15], cross-gain modulation (XGM) [8], [16], cross absorption modulation (XAM) [17], [18], and fast nonlinear polarization switching (NPS) [19]. However, FWM is limited by its low conversion efficiency and wavelength inflexibility [7], [9]. Conversion efficiency is defined as a ratio of the output converted signal power with respect to the input

Manuscript received November 20, 2007; revised June 5, 2008. Current version published February 13, 2009. This work was supported by the European Commission for research activities executed in the FP6 IST-LASAGNE project and FP6 NoE ePhoton/ONe+ program.

N. Yan was with the COBRA Research Institute, Department of Electrical Engineering, Eindhoven University of Technology, 5600 MB Eindhoven, The Netherlands. She is now with the Security and Technology Group, Advisory Business Unit, PricewaterhouseCoopers, 1101 HG Amsterdam, The Netherlands (e-mail: ni.yan@nl.pwc.com).

J. del Val Puente was with the Eindhoven University of Technology, 5600 MB Eindhoven, The Netherlands. (e-mail: finifei@yahoo.es).

E. Tangdiongga and A. M. J. Koonen are with the COBRA Research Institute, Department of Electrical Engineering, Eindhoven University of Technology, 5600 MB Eindhoven, The Netherlands (e-mail: e.tangdiongga@tue.nl; a.m.j.koonen@tue.nl).

T. G. Silveira is with Nokia Siemens Networks Portugal SA, 2720-093 Amadora, Portugal (e-mail: tiago.silveira@nsn.com).

P. Monteiro is with Nokia Siemens Networks Portugal SA, 2720-093 Amadora, Portugal, and also with the Instituto de Telecomunicações Aveiro, 3810-193 Aveiro, Portugal (e-mail: paulo.1.monteiro@nsn.com).

A. Teixeira and A. P. S. Ferreira are with the Instituto de Telecomunicações Aveiro, 3180-193 Aveiro, Portugal (e-mail: teixeira@ua.pt; aferreira@av.it.pt.)

Color versions of one or more of the figures in this paper are available online at http://ieeexplore.ieee.org.

Digital Object Identifier 10.1109/JLT.2008.929093

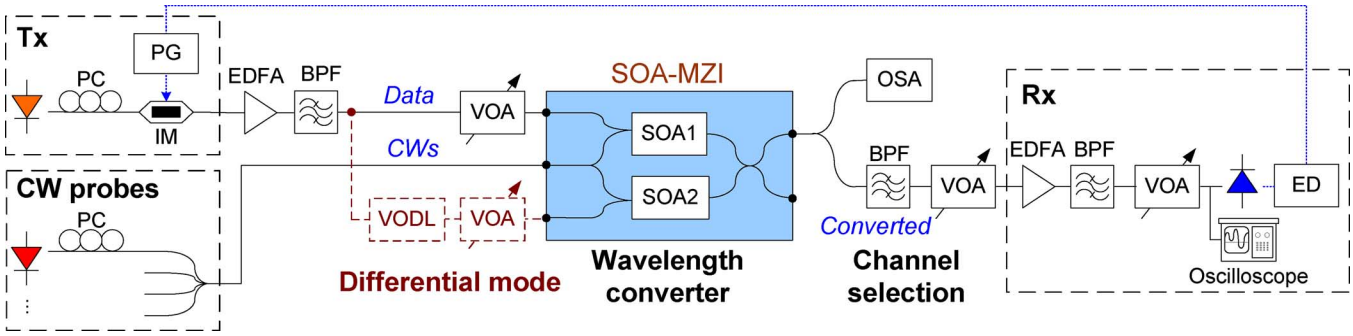

Fig. 1. General setup for simulations and experiments of MWC via a SOA-MZI (IM: intensity modulator; PG: pattern generator; ED: error detector).

signal power [1]. XGM by double-stage SOAs requires high input optical signal power because of the splitting process to both SOAs [8], [16]. XAM suffers from large insertion loss of electroabsorption modulators and only MWC of return-to-zero (RZ) signals has been demonstrated [17], [18]. NPS technique is polarization sensitive, requires high input power and consequently is also penalized by the significant FWM byproducts generated inside the SOA [19].

In comparison, XPM-based multiwavelength converters using a single SOA-MZI excel the others by offering the greatest combination of desirable features, including [12]–[15]: high integrability, satisfactory and flat conversion efficiency, low power consumption, wide conversion bandwidth covering the SOA gain spectrum, simultaneous conversion of a considerable number of channels, wavelength flexibility, commercial product availability, compactness, supporting both RZ and non-return-to-zero (NRZ) data format, possible signal regeneration and noise suppression, and high operation speed. SOA-MZIs also can be deployed with a differential scheme to operate beyond the speed limitation of the SOAs. Moreover, SOA-MZI is a switching element that is widely used in a broad area of applications in optical communications, which allows massive production to reduce the cost. Several SOA-MZIs can be integrated on a single chip. Furthermore, its working principle and schematic are simple and straightforward, requiring no more complexity than any of the other methods reported. MWC can be easily achieved providing a data signal and several continuous waves (CWs) on the desired probe wavelengths to the interferometric ports of a SOA-MZI device.

Previous demonstrations using SOA-MZIs for MWC were reported as individual experiments [4], [12]–[15]. In [12], an additional high optical power assist light was employed for MWC at 10 Gb/s. In [13], differential mode was used for 10 Gb/s operation, and no BER results were shown for 40 Gb/s operation. Moreover, with the unequal channel spacing and large signal detuning deployed in [13], the negative influence of the FWM interference could not be identified and evaluated.

In this paper, we present the first systematic simulation and experimental characterization on the performance and limitations of ITU standard 200- and 100-GHz spaced MWC at 10 Gb/s and 40 Gb/s based on a single SOA-MZI. We analyze the behavior of the MWC regarding the channel performance variations under different parametric conditions. We identify and prove for the first time, that high-order FWM interference is an important performance limiting factor for the maximum number of simultaneously converted channels under equal wavelength spacing. The paper is organized as follows. In Section II, we describe the general setup and explain the operation principle. In Section III, simulations results on SOA-MZI-based MWC are presented and discussed. In Section IV, experimental performance is demonstrated and analyzed. Finally, Section V summarizes and concludes the paper.

II. Setup and Operation Principle

In order to have comparable results, simulation and experimental parameters and configurations for the performance evaluation were largely kept the same, as shown in Fig. 1. In both simulations and experiments, ITU standard channel spacing of 200 or 100 GHz were deployed. Slightly different power levels were applied in simulations and different sets of experimental measurements for characterization and optimization purposes. Regarding the experiments, due to the limited number of laser sources, only one-to-four MWC was investigated. As for the simulations, MWC to four and eight channels were analyzed.

The data signal (Tx) was generated by externally intensity-modulating a CW tunable laser source or a train of optical pulses with a pseudorandom bit sequence (PRBS) to obtain NRZ and RZ signals, respectively. The signals were then optically amplified by an erbium-doped fiber amplifier (EDFA). Four CWs or more were combined and launched in the co-propagating direction with the data signal. Polarization controllers (PCs) were included to adjust the polarization of each channel in order to optimize the performance. Right after the SOA-MZI, an optical spectrum analyzer (OSA) was placed to monitor the output spectrum of the MWC. Finally, the converted wavelength channels were individually selected by an optical bandpass filter (BPF) and detected by a preamplified receiver (Rx) for bit-error rate (BER) tests. The other BPFs in the setup were used to remove the out-of-band amplified spontaneous emission (ASE) noise from the EDFAs. Variable optical attenuators (VOAs) were deployed in several parts of the setup to adjust the optical power to appropriate values. When differential mode was configured, a variable optical delay line (VODL) and a VOA were employed to tune the time and optical power difference between data streams traveling in the upper and lower arms of the MZI.

MWC performance evaluation at both 10 and 40 Gb/s was carried out. At 10 Gb/s, the SOA-MZI was operated in the stan-

TABLE I
PHYSICAL PARAMETERS OF SIMULATED SEMICONDUCTOR OPTICAL AMPLIFIERS IN *VPI* [24]

Parameter	Value		Units
	10 Gb/s	40 Gb/s	
SOA length	1	0.5	mm
SOA width	1	0.3	μm
SOA height	0.2		μm
optical confinement factor Γ	0.3		
fixed internal losses	3000		1/m
differential gain (gain cross section σ_g)	2.8e-20	3e-20	m^2
carrier density at transparency	1.4e24		$1/m^3$
IndexToGainCoupling α	3	1	
linear recombination constant (A)	1.43e8		1/s
biomolecular recombination constant (B)	1.0e-16		m^3/s
Auger recombination constant (C)	1.3e-41	3.0e-41	m^6/s
initial carrier density	2.0e24		$1/m^3$

dard configuration where NRZ-coded data were sent to only one of the two data input ports. Wavelength conversion is obtained through phase shift on the CWs injected into middle port, induced via XPM and the SOA. The MZI translates the phase modulation into an amplitude modulation [20]. As the phase change is only weakly dependent on the wavelength, input data can be simultaneously transferred onto the multiple probe wavelength channels. At 40 Gb/s, the differential mode was employed, shown in Fig. 1 with dashed lines. RZ data format was applied. The differential configuration requires a delayed and attenuated signal traveling in the lower data arm to cancel the broadened converted pulse tails due to the slow SOA recovery time. The output data width and shape are determined by the delay time and the optical power difference between the data signals in the separate arms of the MZI. Due to the random nature of the data pattern, the two data pulse streams require bit-level synchronization.

III. SIMULATION MODELING AND RESULTS

We used *VPItransmissionMaker™ WDM* simulator to carry out simulations of MWC at 10 and 40 Gb/s. The SOA-MZI wavelength converter in *VPI* deploys a standard traveling wave SOA model [21]–[23]. This model assumes a polarization-independent SOA that can handle signals with arbitrary polarization states. Besides, this model neglects SOA gain dispersion and internal ASE noise. Table I summarizes the physical parameters of the simulated SOAs in *VPI*.

Neglecting *SOA gain dispersion* means that the SOA gain spectrum is independent of the wavelength. This is valid as long as the spectrum occupied by the optical signals falls within the amplification bandwidth. Typically, the SOA amplification bandwidth is in the order of several tens of nanometers. Most standard SOAs have a gain spectrum of around 30 nm when used as wavelength converters. This sets one limitation on the maximum possible number of channels for MWC, because the input data signal and the CW probes to be injected into the SOA-MZI must be within this range. For our simulations with up to eight channels at 200-GHz channel spacing, this condition is always fulfilled.

TABLE II
SIMULATION PARAMETERS

Data Rate	Channel Configuration	I_{bias} (mA)		P_{in} (dBm)	
		SOA1	SOA2	Data1/2	CW Total
10 Gb/s	200 GHz / 4CH	313	281	-1	0
	200 GHz / 8CH	300	270		
	100 GHz / 4CH	350	320		
40 Gb/s	200 GHz / 4-8CH	300	305	6.5/0.5	7

The *SOA internal ASE noise* is important but not critical for the noncascading MWC of up to eight channels that we simulated, although neglecting the ASE noise can result in overoptimistic estimation of the optical signal-to-noise ratios (OSNRs). ASE can be critical in systems where several ASE sources are cascaded, in which case the degraded OSNRs of the optical signals can affect significantly the correct detecting of the signals at the receiver; or when a higher number of MWC channels are present, where the signal power level per channel is considerably lower but the noise power level remains the same.

The longest available PRBS signal pattern length in *VPI* is $2^{23}-1$, which was deployed in all simulations. Other simulation parameters are summarized in Table II.

A. MWC Simulations at 10 Gb/s

The VPI simulation schematic for MWC at 10 Gb/s follows the standard configuration illustrated in Fig. 1. The simulation schematic utilizes an externally modulated *transmitter* for the original data channel and a variable number of CW lasers multiplexed into the central port of the SOA-MZI as the probe channels. At the output of the SOA-MZI, the simultaneously converted channels were separated by a basic *demultiplexer* in *VPI*, which is an attenuator with standard third-order filters configured with 40 GHz bandwidth. After demultiplexing, each converted channel was amplified by an EDFA, and then filtered by a BPF to remove the out-of-band ASE noise. Finally, the signals were sent to three different modules: i) an *ideal optical to electrical converter* followed by an *electrical signal analyzer* that calculates the eye extinction ratio (ER) illustrated in a *text visualizer*; ii) a *BER measuring block* together with a *power meter* for measuring BER versus received optical power; iii) a *clock recovery circuit* followed by a *scope* for eye pattern visualization. The outputs of all the *BER* modules, including one for the original signal channel, were plotted in an *XY visualizer* to generate the BER curves.

In all the simulations at 10-Gb/s bit rate, the original signal channel wavelength was set to 1541.35 nm. The detuning of the CW channel that was closest to the signal channel was 400 GHz. The injection current to SOAs was optimized for each set of measurements, shown in Table II.

1) 200-GHz Channel Spacing, One-to-Four MWC: Fig. 2(a) presents the simulated output spectrum of the MWC. The data in the original signal channel were copied onto all the CW probe wavelength channels. The SOA-MZI showed good conversion efficiency, because of the gain provided by the SOAs and the fact that the SOA-MZI converts phase modulation into amplitude modulation.

From Fig. 2(a), several FWM contributions due to the SOA nonlinear effect can be seen aside the input channels. Although

the out-of-band FWM satellite signals were significantly weaker than the MWC channels, the existence of the in-band FWM products affected the performance of the MWC channels, which consequently influenced their BER performance and eye opening, shown in Fig. 2(b) and (c). These FWM components, which carry exactly the same data as the desired channels, were generated inside the bandwidth of each converted channel. In experiments, such FWM interference can be minimized by adjusting the polarizations of the input channels because FWM phase matching conditions are strongly polarization dependent.

In Fig. 2(b), the BER results of the four converted channels as well as the original input channel are plotted. As we can see, the negative impact of the FWM byproducts on the four-channel MWC performance was not very pronounced, for the maximum power penalty among the four channels was around 0.5 dB. Nevertheless, the larger power penalties were related to the channel 1 (Ch1) and channel 4 (Ch4), the two outer channels that suffer most from the in-band FWM crosstalk. These undesired FWM components reduced the upper part of the eye opening of the converted channels and, therefore, caused eye distortion at the logical *one* level of the converted channels, especially that of the outer channels. The consequence of such distortion was that the converted eye diagrams had an obviously *thicker one* level, which is exhibited in the Ch1 eye diagram inset in Fig. 2(b).

In Fig. 2(c), the ERs, power penalties and Q factors of the converted channels are presented. Note that due to the fact that in an ideal simulation environment, there is no external influence such as noise and temperature fluctuations, or hardware imperfections such as loss and reflections, the absolute values of the ERs and Q cannot represent the performance of the system in realistic conditions. However, the relative values of these parameters can reflect channel- and simulation configuration-dependent performance characteristics, because free from other impacts, the simulation results reveal primarily the effects of the nonlinear interactions in the system.

Fig. 2(c) confirmed that the outer channels had worse eye quality. Nevertheless, all the four channels exhibited clear and open eye diagrams, which agrees with the error-free operation of the MWC and the low power penalties achieved.

2) 200-GHz Channel Spacing, One-to-Eight MWC: Fig. 2(d) presents the output spectrum. The output OSNRs were still high but the FWM satellite signals were much stronger now that there were more interacted channels. From the BER results in Fig. 2(e) and channel parameters in Fig. 2(f), it was observed that the impact of the in-band FWM products was also severer. Not only the power penalty of Ch1 increased to more than 1 dB, but a slight error floor also appeared in Ch1. Comparing to the second worst channel, Ch8, Ch1 had an extra 0.5 dB penalty at the BER of 10^{-9}. Moreover, from the eye diagrams presented in Fig. 2(f), Ch1 suffered more from the FWM contributions. This is because Ch1 was the closest channel to the high-power modulated input data channel, and, thus, more higher-order FWM byproducts were generated inside the bandwidth of Ch1, which resulted in a higher degree of eye closure and distortion.

Fig. 2(f) reveals the same channel characteristics observed in the one-to-four MWC, that the outer channels had worse quality than the central channels with respect to the Q values and power penalty. The ERs of the converted channels were not affected by the FWM contributions, though on average the ERs were slightly lower than those in the four-channel case.

3) 100-GHz Channel Spacing, One-to-Four MWC: Simulations were carried out with reduced channel spacing of 100 GHz. Fig. 2(g) presents the output spectrum. With signal detuning still kept at 400 GHz, there are more FWM satellite signals due to the halved channel spacing. The BER results in Fig. 2(h) indicated obvious error floors in all the four channels, with the simulated power penalty increased to 2–4 dB at the BER of 10^{-9}. The eye patterns and channels parameters in Fig. 2(i) show higher degrees of degradation due to stronger nonlinear interactions, which can explain the higher power penalty and the BER floor obtained. The behavior of the channels is in accordance with the observations from the previous simulations, but the simulated values of ERs and Q were much lower. By reducing the input power of the data signal and the CW probes, the performance of the 100-GHz spaced MWC could be in principle improved, but the power penalties were still larger than those in the 200-GHz cases.

As the simulations results of the 100 GHz were not as satisfactory as with 200-GHz spacing, we did not further increase the number of channels.

4) Unequal Channel Spacing, One-to-Eight MWC: To confirm our observations from the previous simulations that FWM interference is one of the major limiting factors of MWC channel performance, another simulation was carried out where eight CW probes with unequal channel spacing were deployed. The channel spacing between adjacent channels were reduced by a step of 25 GHz from 250 GHz between Ch1 and Ch2. The output spectrum, shown in Fig. 3(a), indicates that numerous FWM products were generated. Due to the unequal channel spacing, most of them fell outside the MWC channel bandwidth.

Fig. 3(b) compares the channel performance variations in terms of Q factor, between the case with unequal channel spacing and 200 GHz channel spacing as presented earlier in Fig. 2(f). It can be clearly observed that the eye diagrams of all the channels look much cleaner, as the FWM interference under unequal channel spacing is greatly reduced. However, although the strong interference from the first-order FWM products are now out of band and can be removed by filtering, from the eye diagrams, we can see that the converted channels are still influenced by some high-order FWM products. The thickened logical *one* level is more pronounced in the channels where the channel spacing is smaller, because under less channel spacing, the FWM interactions are stronger and the high-order FWM products generated are also stronger. The Q factor trend suggests that under unequal channel spacing, the quality of the converted eye diagrams are higher. The Q factor is strongly affected by the channel spacing and the position of the channels.

B. MWC Simulations at 40 Gb/s

40 Gb/s MWC based on this SOA-MZI model had to be carried out under differential mode in order to avoid the effects of the SOA carrier dynamics [13]. In the differential VPI simulation scheme, a *pulse Gaussian transmitter* was used as a data generator to produce the 40-Gb/s RZ pulse train. The full width at half maximum (FWHM) of the RZ source pulse was around 2 ps. Push

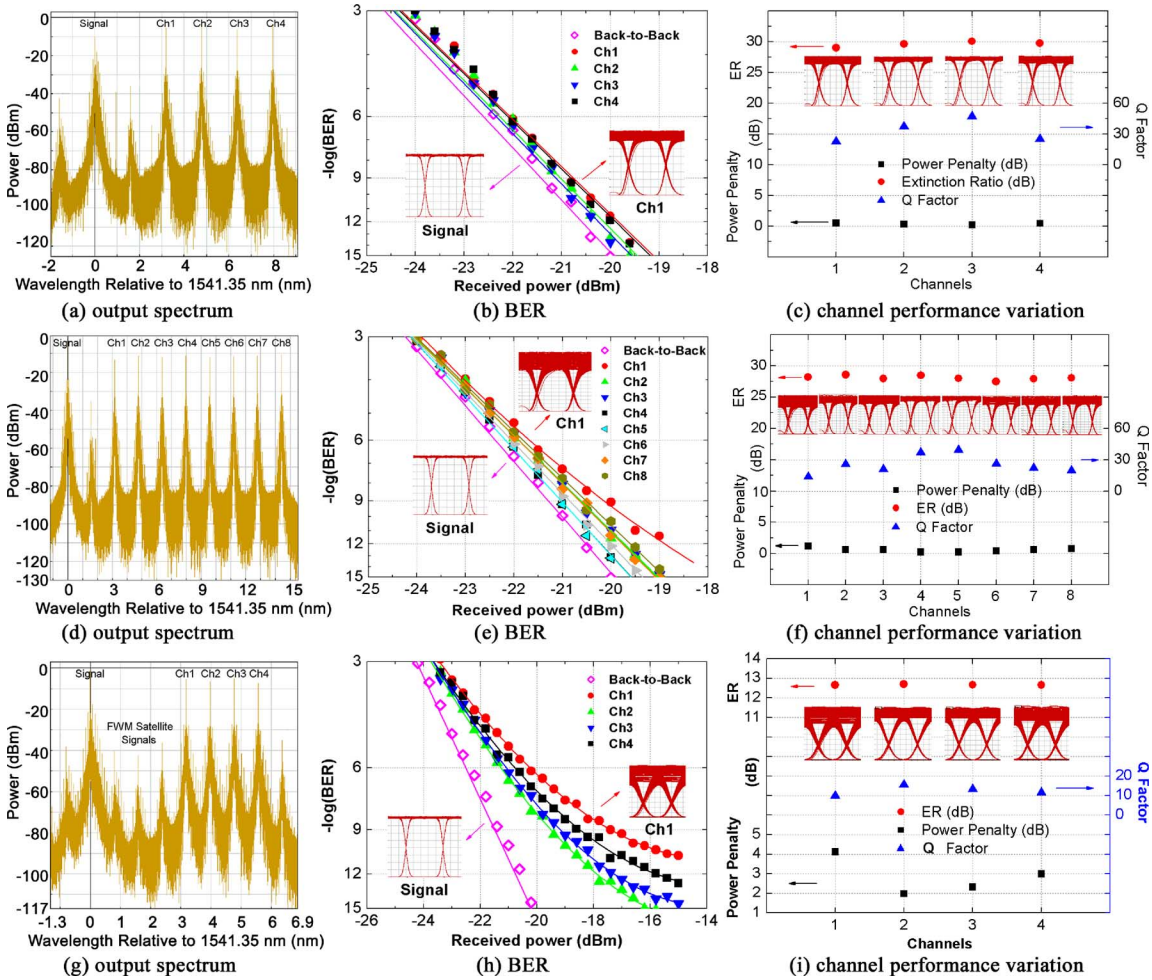

Fig. 2. Simulation results at 10 Gb/s: (a)–(c) 200-GHz spacing, four channels; (d)–(f) 200-GHz spacing, eight channels; (g)–(i) 100-GHz spacing, four channels.

data pulses were sent into one arm of the MZI inducing a nonlinear phase shift within the SOA. This nonlinearity was offset by inducing a similar effect within the SOA of the other arm by delayed pull pulses. All the filters were configured with 130-GHz bandwidth to accommodate the wide 40 Gb/s RZ spectrum. Each extracted and preamplified channel was sent to a *scope* for eye pattern visualization. At 40 Gb/s, we did not obtain any numerical estimation on the MWC performance in terms of BER measurement because *VPI* did not yield any results with the differential configuration when the same *VPI* measurements building blocks as used in the simulations at 10 Gb/s were applied.

In these simulations, the original signal channel wavelength was set to 1556 nm. 400-GHz signal detuning and 200-GHz CW channel spacing were used. For 40-Gb/s RZ signals, these minimum spectral spacings between the adjacent channels are necessary to avoid significant interchannel crosstalk. The corresponding delays on the two data paths were 4 and 10 ps, respectively. In the simulations, a minimum power difference of 6 dB between the two data paths was required to enable the proper operation of the differential mode, while increasing the power difference up to 10 dB did not have any visible influence on the switching performance based on eye pattern observation.

1) One-to-Four MWC: The spectrum obtained at the output of the SOA-MZI is presented in Fig. 4(a). The simulated RZ spectra of the converted channels are difficult to distinguish because of all the RZ discrete spectral tones at multiples of the clock frequency. However, the eye diagrams of the MWC signals, shown in Fig. 4(b), are clear and open. The FWHM of the MWC channels are 5–6 ps. The duration of the tailing edges of the converted pulses depends on the effective carrier lifetime of the SOAs. Due to the slow carrier dynamics of the SOAs, the tailing edges are longer than the rising edges. In this case, when differential mode is used, the pulse shape depends on the amplitude and delay difference between the data signals traveling in the upper and lower arms of the MZI. By adjusting these two parameters, one can obtain narrower pulses. However, because of the slow carrier dynamics of the SOAs and the limited granularity and accuracy of the fiber delay lines, it is not possible to achieve the same or a similar pulse shape and a 2-ps width as the original input RZ pulses.

As in the previous 10-Gb/s simulations with NRZ signals, we again perceived the FWM influence in degrading the outer channels (Ch1 and Ch4).

2) One-to-Eight MWC: The eye patterns for one-to-eight MWC shown in Fig. 4(d), are still clear and open. As before, the bordering channels were more affected by the in-band FWM byproducts, especially the channel that was closest to the input signal wavelength (Ch8).

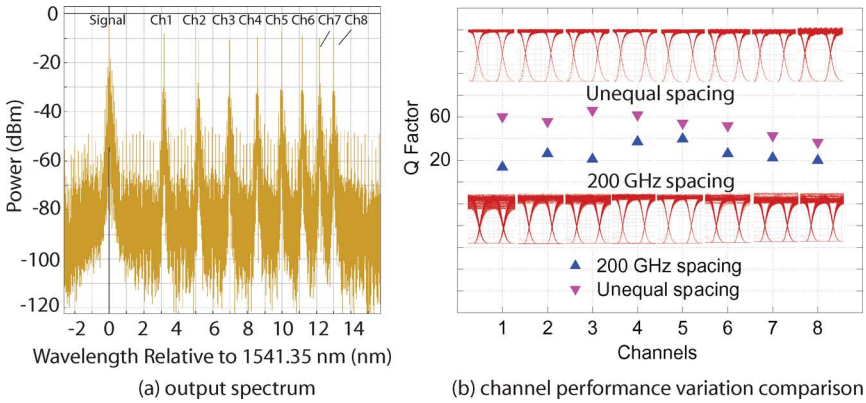

Fig. 3. Simulation results at 10 Gb/s: unequal channel spacing.

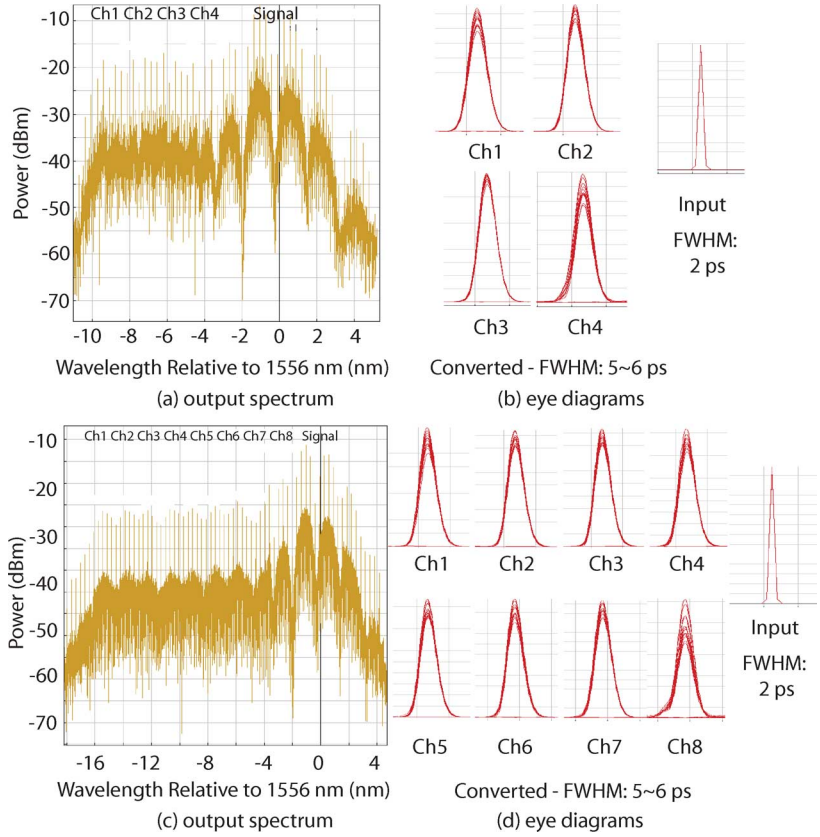

Fig. 4. Simulation results at 40 Gb/s: (a), (b) four channels; (c), (d) eight channels.

C. Discussions on Simulation Results

The presented simulation results indicate good feasibility of employing a SOA-MZI for MWC applications such as optical layer data multicast. At 10 Gb/s, the simulated power penalties were small, with clear and open converted eye patterns. At 40 Gb/s, widely open eye diagrams were also obtained with differential operation.

The observations in all the simulations lead to the following conclusions. i) With increased number of channels and reduced channel spacing, the performance of the MWC tends to decrease. ii) Individual channel performance is strongly influenced by the in-band high-order FWM products, which is related to the position of the channel among all the input wavelengths. In general, the outer converted channels have the worse performance, with the two bordering channels suffering most from the FWM interference. Usually the MWC power penalty gradually decreases from the channel that is furthest from the input data channel, to a minimum value around the central channel, and then gradually increases again until it reaches a maximum value for the channel that is closest to the data signal. The Q factors of all the converted channels follows the opposite trend to that of the power penalty. iii) The in-band FWM byproducts degrade the converted eye diagrams by lowering the eye opening due to the crosstalk they introduce to the desired MWC channels; therefore, the influenced eye patterns have a thickened logical *one* level. However, such high-order FWM interference does not affect the ERs of converted signals. Therefore, the ERs of all the

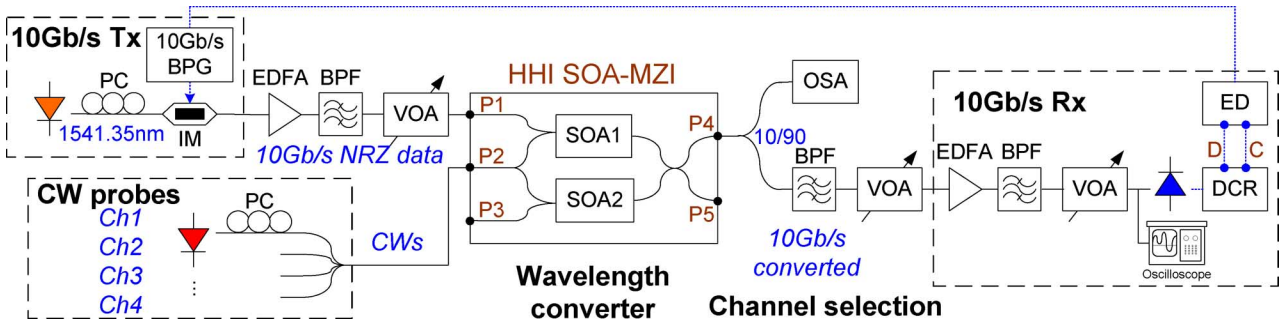

Fig. 5. Experimental setup of MWC via a SOA-MZI at 10 Gb/s.

TABLE III
EXPERIMENTAL PARAMETERS

Data Rate	Channel Configuration	I_{bias} (mA) / θ (V)		Ave. P_{in} (dBm)	
		SOA1	SOA2	Data1/2	CW Indiv.
10 Gb/s	200 GHz / P5	283.11	282.17	0.3	-6
	100 GHz / P5	323.60	312.50	-1.1	
	100 GHz / P4	242.96	310.95	-1.2	
40 Gb/s	600 GHz det.	400/7.8	400/0	7.3/-3.0	3.3∼6.1
	700 GHz det.	400/8.0	400/0	11.6/1.3	3.4∼5.0

converted channels generally retain a certain level if all input CW probes are injected with uniformed optical power.

IV. EXPERIMENTAL CHARACTERIZATION AND RESULTS

In order to validate the feasibility and assess the lab performance of SOA-MZI-based MWC, experiments at both 10 and 40 Gb/s were carried out. All components employed in the experimental setups, including the integrated SOA-MZIs, are commercially available. In all experiments, ITU standard 200- or 100-GHz spaced wavelengths were deployed. The input data signal was configured with PRBS of pattern length $2^{31}-1$. Both SOA-MZIs we used were for 10-Gb/s standard operation speed. Other experimental parameters are summarized in Table III.

A. MWC Experiments at 10 Gb/s

Fig. 5 shows the experimental setup for the 10-Gb/s MWC demonstration, where all-optical wavelength multicast via a SOA-MZI was achieved by launching a data signal and four CWs on the desired wavelength channels to the interferometric ports of the device. The monolithically integrated SOA-MZI wavelength converter was manufactured by Heinrich Hertz Institut (HHI). Both SOAs were 1-mm long. The NRZ data signal was generated by externally modulating a tunable CW laser source tuned to 1541.35 nm. Four 200/100 GHz spaced CWs starting from 1544.53 nm were combined by a four-to-one coupler and launched in the co-propagating direction with the data signal. The total input power to P2 was around 0 dBm at the output of the coupler with each individual CW channel alone adjusted to about -6 dBm. At the SOA-MZI output ports, a BPF of 0.3 nm narrow bandwidth was used for the channel selection. Simultaneously wavelength converted channels were obtained at both arms P4 and P5, and sent for the BER test. All the BER measurements, including the back-to-back one, were performed under the same threshold level.

1) 200-GHz Channel Spacing, Output P5: Fig. 6(a) presents the output spectrum. The input signal had an ER of 12.33 dB. Its OSNR before the VOA was 56 dB, measured by an OSA with 0.01-nm resolution bandwidth. The output OSNRs for the converted channels were within the range of $40 \sim 43$ dB. The spectrum revealed a 3.4-dB average peak power ratio of the individual converted channels to the signal channel after the SOA-MZI MWC. Out-of-band FWM components were at least 25-dB weaker than the desired channels. Although the in-band FWM products were expected to be much stronger, their negative influence on the BER performance was negligible, as shown in Fig. 6(b). The power penalties of the four channels at $\mathrm{BER} = 10^{-9}$ were within the range of $0.14 \sim 0.39$ dB.

The main reason that the experimental results were better than those in the simulations is that the SOA model in the simulations is insensitive to the signal polarizations; however, in experiments, it is possible to optimize the output channel performance by adjusting the incoming signal polarizations so that the FWM degradation is minimized.

Fig. 6(c) demonstrates the output eye signal-to-noise ratios (S/N) and ERs of the four simultaneously converted channels including their eye diagram snapshots, measured by an oscilloscope with 40-GHz bandwidth limit. All the channels showed clear and widely open eyes with eye S/N's ranging from 8.50 for Ch1 to 11.27 for Ch4, and an average ER of 10.76 dB.

2) 100-GHz Channel Spacing, Output P5: The input signal and the converted channel OSNRs were 55 dB and $40 \sim 41$ dB, respectively. The input ER was 14.18 dB. After reducing the channel spacing to 100 GHz, as shown in Fig. 6(d), the MWC did not exhibit noticeable BER performance degradation, plotted in Fig. 6(e). The converted channels had negligible negative power penalties of $0.04 \sim 0.30$ dB at $\mathrm{BER} = 10^{-9}$. The eye patterns insets in Fig. 6(f) are still clear. However, compared to the 200 GHz spaced MWC, we observed a slightly smaller eye opening and more noise at both *zero* and *one* levels. The measured eye S/N's were lower, starting from 6.92 for Ch1 to 8.62 for Ch4. This is due to the stronger in-band FWM interference, a drawback of placing the channels closer to each other. The average ER of the converted channels was 10.49 dB.

3) 100-GHz Channel Spacing, Output P4: In this experiment, we degraded the input signal OSNR to 21 dB. The input

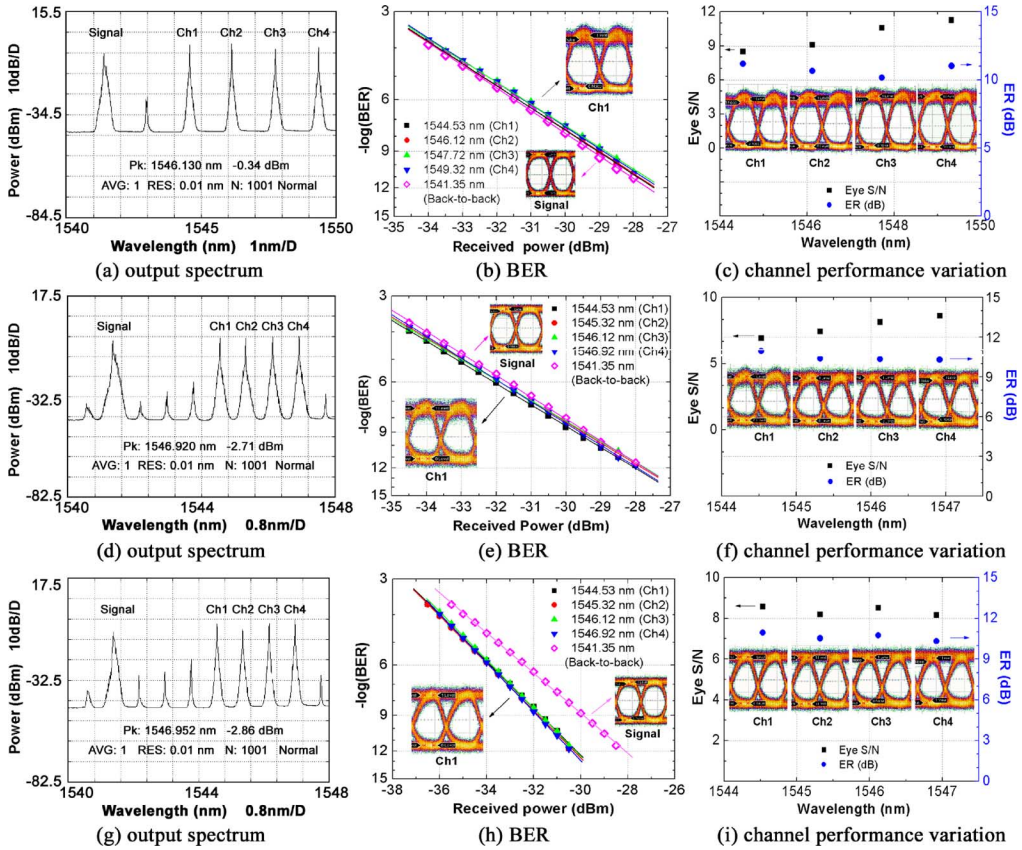

Fig. 6. Experimental results at 10 Gb/s: (a)–(c) 200-GHz spacing, output P5; (d)–(f) 100-GHz spacing, output P5; (g)-(i) 100-GHz spacing, output P4.

ER was 13.03 dB. All the BER measurements, including the back-to-back one, were performed keeping constant power of 0 dBm to the photo detector (PD). Even with the degraded input signal, the MWC channels at the output still had high OSNRs of $38 \sim 43$ dB, as shown in Fig. 6(g), with on average 20-dB enhancement over the input signal OSNR. The SOA-MZI increased the signal quality by suppressing the noise power in the converted signals, because of its nonlinear transfer function due to the phase difference in the interferometric arms [25]. The average peak power ratio of the individual converted channels to the signal channel after the SOA-MZI MWC was 4 dB. At the receiver, the peak power ratio of the neighboring channels that were not completely suppressed by the filters to the selected channel was about -33 dB. As regards to the observed OSNR improvement, the SOA-MZI appears as a promising device for regeneration applications.

In Fig. 6(h), the BER values confirmed that the input data was converted to all the four channels with a receiver sensitivity improvement of 1.84 dB or more, while the sensitivity divergence among the four converted channels was measured to be no more than 0.14 dB. The BER results, in addition to the OSNR improvement, indicated that this SOA-MZI could be an attractive device for regeneration purposes.

In Fig. 6(i), all the channels showed clear and widely open eyes with an average eye S/N of 8.36 and an average ER of 10.63 dB. The clean multicast channels depicted by the eye snapshots further proved the excellent performance of the MWC for WDM applications.

B. MWC Experiments at 40 Gb/s

The experimental setup for 40 Gb/s is shown in Fig. 7. MWC was achieved by a hybrid integrated SOA-MZI twin regenerator from the Centre of Integrated Photonics (CIP). The SOAs are multiquantum well devices with saturated response time below 30 ps. The 40-Gb/s RZ data of 2-ps pulse width was generated by modulating a 40-GHz ultrafast optical clock (UOC) using a Mach–Zehnder modulator (MZM) with 40-Gb/s PRBS. An EDFA was used to compensate for the power loss in the modulation process. The data signal was tapped onto both of the SOA-MZI arms *A* and *D* using a 50/50 coupler, with the lower data path delayed by a VODL to achieve the differential mode. Four 200-GHz spaced CWs at wavelength $1547.72 \sim 1552.52$ nm were combined by a multiplexer and injected in the co-propagating direction into SOA-MZI port *B*.

Both SOAs were pumped with 400 mA maximum allowed current to facilitate fast recovery time, while in the upper arm a phase shifter (PS) after the SOA1 was controlled with a voltage to obtain noninverted output at MZI output *J*. After MWC, the converted data signals were demultiplexed and individually fed to a preamplified receiver and an ED. The -3 dB bandwidth of all the optical filters including the (de)multiplexers was 130 GHz. For the BER measurement, signal OSNR was degraded at the PD input by increasing the ASE noise level while keeping the signal power constant at -1 dBm to ensure linear operation of the electrical circuitry. The OSNR was taken using an inline power meter before the PD by disabling sequentially

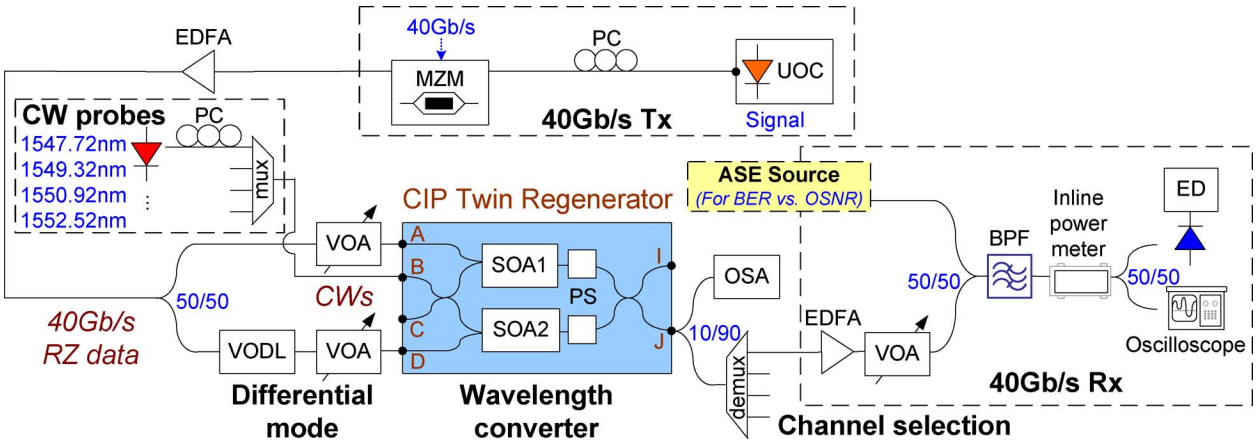

Fig. 7. Experimental setup of MWC via a SOA-MZI at 40 Gb/s.

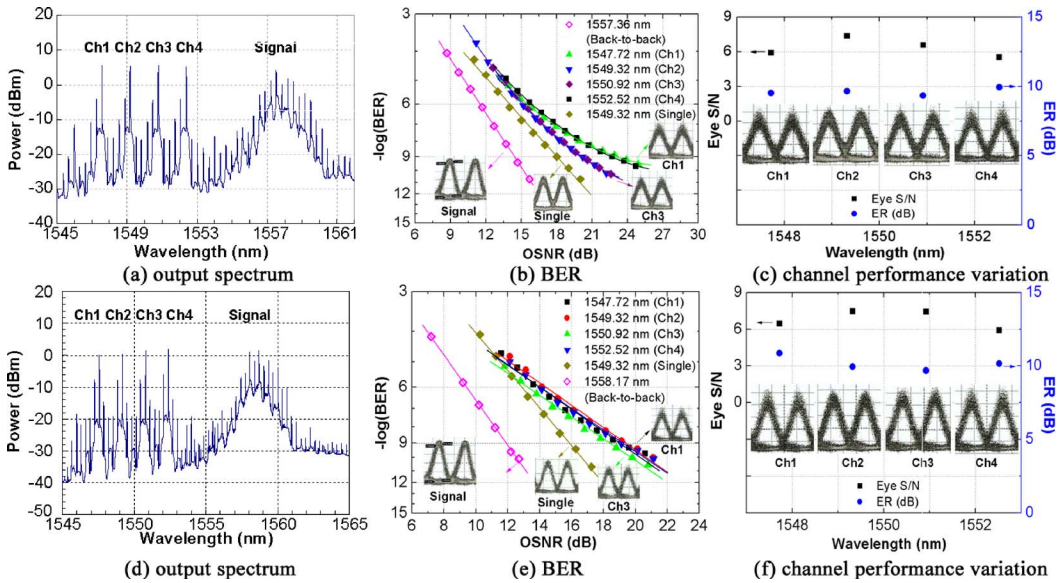

Fig. 8. Experimental results at 40 Gb/s: (a)–(c) 600-GHz data detuning; (d)–(f) 700-GHz data detuning.

the signal or the ASE. The receiver had an electrical bandwidth of 37 GHz.

1) 600 GHz Detuning: The 2-ps pulse source from the UOC was tuned to 1557.36 nm. The differential delay between the two data streams was around 6.5 ps. Fig. 8(a) shows the output spectrum. The FWM satellite signals at both sides of the converted channels were at least 17-dB weaker. In Fig. 8(b), the BER is plotted as a function of the OSNR at the PD input for the MWC channels, back-to-back reference as well as a single wavelength conversion (SWC). We observed 3.6-dB OSNR penalty at BER of 10^{-9} for the SWC to 1549.32 nm. The penalty was mostly due to the pulse broadening caused by the slow SOA gain recovery time, which could not be completely canceled via the differential configuration. The MWC channels demonstrated a minimum 2-dB OSNR penalty with regard to the SWC. Ch1 and Ch4 also had a slight error floor, which caused the OSNR sensitivity variation of another 3 dB at BER of 10^{-9} from the two central channels. The worse performance of the outer channels due to the in-band FWM interference can also be observed from the eye snapshots presented in Fig. 8(c). The average ER for the four channels was 9.61 dB, with the largest ER difference among two different channels no greater than 0.61 dB.

2) 700-GHz Detuning: To reduce the crosstalk from the input signal, a second set of measurements was made with the data channel moved to 1558.17 nm. The lower data path was delayed for 7.6 ps. Fig. 8(d) presents the output spectrum. The out-of-band FWM by-products were more than 20 dB weaker. Fig. 8(e) shows all the BER curves. The average OSNR penalties of the MWC channels at BER equal to 10^{-9} were 3.5-dB relative to the SWC, and 7 dB to the back-to-back reference. In this experiment, less than 1-dB OSNR sensitivity difference among all the MWC channels was achieved and no error-floor was observed. In Fig. 8(f), clear eye opening can be seen. The oscilloscope measured an average ER of 10.16 dB for the MWC channels, with the worst being 9.68 dB.

C. Discussions on Experimental Results

Our experimental results confirmed previous observations in simulations, and proved the promising performance of all-optical MWC by XPM in a SOA-MZI. We achieved error free

operation and obtained clear, open eye diagrams and negligible performance difference among all the MWC channels at both 10 and 40 Gb/s. Under the investigated experiment configurations, the FWM byproducts did not seem to be a limiting factor for the maximum number of channels, nor for the deployed channel spacing. By increasing the number of CW probes or reducing their channel spacing, the demonstrated schemes can accommodate more channels. With faster SOA dynamics, such MWC setups can operate at higher bit rates.

However, unlike in simulations, experimental results are influenced by various optical and electrical noises, and the total CW power to the SOA-MZI is constrained by the maximum input power limit of the device. When increasing the number of CW channels, the optical power of each channel may need to be reduced accordingly, and, thus, the performance of each channel declines. Therefore, under realistic circumstances, the maximum number of MWC channels is decided by acceptable performance of all the channels under the combination of the following conditions: i) the allowed total input CW power to the device, usually no more than 10 dBm; ii) SOA gain spectrum, with typical usable bandwidth of less than 30 nm; iii) deployed channel spacing, depending on the data bit rate and modulation format.

V. Summary and Conclusions

We present for the first time, extensive simulation and experimental characterizations of single SOA-MZI-based MWC at both 10 and 40 Gb/s bit rates. Our results confirmed its promising performance with standard ITU channel spacings for WDM applications in future high capacity, high transparency optical networks. Moreover, we analyzed and discussed MWC system performance as well as channel-specific performance under different parametric conditions. Finally, we identified and summarized the major restrictions on the maximum number of MWC channels and their wavelength configurations.

Our experimental results at 10 Gb/s revealed signal regeneration possibilities of a SOA-MZI for MWC. This feature is particularly desirable for WDM network nodes as in practice, optical crossconnects inside a network often do not receive clean input signals directly from the source, but degraded optical data channels with impaired OSNRs due to cascaded optical amplifiers they have passed through across long distances. Optical signal regeneration capabilities thus improve the quality of the incoming data to allow for further propagation in the optical layer without the necessity of OEO conversion and electronic regeneration.

In optical networks, the cascadability of the MWC scheme for wavelength multicast generally depends on the number of MWC channels, the bit rate and the properties of employed SOA-MZI devices. In our experiments, the same setup at 10 Gb/s is expected to be able to cascade without much additional penalties. At 40 Gb/s, the cascadability of the tested CIP device is not very good, so additional penalties are expected if the differential MWC setup is to be cascaded.

SOA-MZIs are used for various functionalities and can be massively produced and integrated to reduce cost. Based on our results, we believe that single SOA-MZI-based MWC can be suitable for various applications in next generation all-optical infrastructures, where optical layer wavelength multicast is a most desirable feature for the increasing volume of multimedia on-demand data services.

References

[1] S. J. B. Yoo, "Wavelength conversion technologies for WDM network applications," *IEEE/OSA J. Lightw. Technol.*, vol. 14, no. 6, pp. 955–966, Jun. 1996.

[2] J. M. H. Elmirghani and H. T. Mouftah, "All-optical wavelength conversion: Technologies and applications in DWDM networks," *IEEE Commun. Mag.*, pp. 86–92, Mar. 2000.

[3] Y. Liu, E. Tangdiongga, Z. Li, H. de Waardt, A. M. J. Koonen, G. D. Khoe, and H. J. S. Dorren, "Error-free 320 Gb/s SOA-based wavelength conversion using optical filtering," presented at the Optical Fiber Comm. Conf., Anaheim, CA, Mar. 2006, PDP28.

[4] N. Yan, T. Silveira, A. Teixeira, A. Ferreira, E. Tangdiongga, P. Monteiro, and A. M. J. Koonen, "40 Gb/s wavelength multicast via SOA-MZI and applications," *IET Electron. Lett.*, vol. 43, no. 23, pp. 1300–1300, Nov. 2007.

[5] N. Yan, A. Alcaide, J. M. D. Mendinueta, E. Tangdiongga, and A. M. J. Koonen, "Cost reduction and traffic performance improvement using direct forward optical layer multicast in optical label switching nodes," in *Proc. European Conf. Optical Comm.*, Berlin, Germany, Sep. 2007, vol. 2, pp. 39–40, 3.2.2.

[6] A. M. J. Koonen, N. Yan, J. J. Vegas Olmos, I. Tafur Monroy, C. Peucheret, E. van Breusegem, and E. Zouganeli, "Label-controlled optical packet routing – Technologies and applications," *IEEE J. Sel. Topics Quant. Electron.*, vol. 13, no. 5, pp. 1540–1549, Sep./Oct. 2007.

[7] G. Contestabile, M. Presi, and E. Ciaramella, "Multiple wavelength conversion for WDM multicasting by FWM in an SOA," *IEEE Photon. Technol. Lett.*, vol. 16, no. 7, pp. 1775–1777, Jul. 2004.

[8] B. H. L. Lee, R. Mohamad, and K. Dimyati, "Performance of all-optical multicasting via dual-stage XGM in SOA for grid networking," *IEEE Photon. Technol. Lett.*, vol. 18, no. 11, pp. 2215–2217, Nov. 2006.

[9] N. Yan, A. Teixeira, T. Silveira, G. M. Tosi Beleffi, F. Curti, D. Forin, F. Dalla Longa, I. Tafur Monroy, P. Monteiro, and A. M. J. Koonen, "Theoretical and experimental performance evaluation of all-optical multi-wavelength conversion by four-wave mixing in fiber at 10/20/40 Gb/s for optical layer multicast," *Micro. Opt. Technol. Lett.*, vol. 49, no. 5, pp. 1067–1071, May 2007.

[10] M. Karasek, J. Kanka, P. Honzatko, J. Vojtech, and J. Radil, "10 Gb/s and 40 Gb/s multi-wavelength conversion based on nonlinear effects in HNLF," in *Proc. Int. Conf. Transparent Optical Networks*, Nottingham, U.K., Jun. 2005, pp. 155–161, Tu.D1.7.

[11] J. L. Pleumeekers, J. Leuthold, M. Kauer, P. G. Bernasconi, C. A. Burrus, M. Cappuzzo, E. Chen, L. Gomez, and E. Laskowski, "All-optical wavelength conversion and broadcasting to eight separate channels by a single semiconductor optical amplifier delay interferometer," in *Proc. Optical Fiber Comm. Conf.*, 2002, pp. 596–597, ThDD4.

[12] H. S. Chung, R. Inohara, K. Nishimura, and M. Usami, "All-optical multi-wavelength conversion of 10 Gbit/s NRZ/RZ signals based on SOA-MZI for WDM multicasting," *IET Electron. Lett.*, vol. 41, no. 7, pp. 432–433, Mar. 2005.

[13] D. Reading-Picopoulos, F. Wang, Y. J. Chai, R. V. Penty, and I. H. White, "10 Gb/s and 40 Gb/s WDM multi-casting using a hybrid integrated Mach–Zehnder interferometer," presented at the Optical Fiber Comm. Conf., Anaheim, CA, Mar. 2006, OFP2.

[14] N. Yan, H.-D. Jung, I. Tafur Monroy, H. de Waardt, and T. Koonen, "All-optical multi-wavelength conversion with negative power penalty by a commercial SOA-MZI for WDM wavelength multicast," presented at the Optical Fiber Comm. Conf. (OFC), Anaheim, CA, Mar. 2007, JWA36.

[15] N. Yan, T. Silveira, A. Teixeira, A. Ferreira, E. Tangdiongga, P. Monteiro, and A. M. J. Koonen, "40 Gb/s all-optical multi-wavelength conversion via a single SOA-MZI for WDM wavelength multicast," in *Proc. Optoelectronics and Communications Conf.*, Yokohama, Japan, Jul. 2007, pp. 530–531.

[16] G. Contestabile, N. Calabretta, R. Proietti, and E. Ciaramella, "Double-stage cross-gain modulation in SOAs: An effective technique for WDM multicasting," *IEEE Photon. Technol. Lett.*, vol. 18, no. 1, pp. 181–183, Jan. 2006.

[17] L. Xu, N. Chi, K. Yvind, L. J. Christiansen, L. K. Oxenløwe, J. Mørk, P. Jeppesen, and J. Hanberg, "8 × 40 Gb/s RZ all-optical broadcasting utilizing an electroabsorption modulator," presented at the Optical Fiber Comm. Conf., Los Angeles, CA, Feb. 2004, MF71.

[18] K. K. Chow and C. Shu, "All-optical signal regeneration with wavelength multicasting at 6×10 Gb/s using a single electroabsorption modulator," *OSA Opt. Exp.*, vol. 12, no. 13, pp. 3050–3054, 2004.
[19] G. Contestabile, N. Calabretta, M. Presi, and E. Ciaramella, "Single and multicast wavlength conversion at 40 Gb/s by means of fast nonlinear polarization switching in an SOA," *IEEE Photon. Technol. Lett.*, vol. 17, no. 2, pp. 2652–2654, Dec. 2005.
[20] D. Wolfson, A. Kloch, T. Fjelde, C. Janz, B. Dagens, and M. Renaud, "40-Gb/s all-optical wavelength conversion, regeneration, and demultiplexing in an SOA-based all-active Mach–Zehnder interferometer," *IEEE Photon. Technol. Lett.*, vol. 12, no. 3, pp. 332–334, Mar. 2000.
[21] A. A. M. Saleh, "Nonlinear models of travelling-wave optical amplifiers," *IET Electron. Lett.*, vol. 24, pp. 835–837, 1988.
[22] S. Shimada and H. Ishio, *Optical Amplifiers and Their Applications*. Chichester, U.K.: Wiley, 1994, ch. 3.
[23] G. P. Agrawal and N. K. Dutta, *Long-Wavelength Semiconductor Lasers*. New York: Van Nostrand Reinhold, 1986.
[24] J. del Val Puente, N. Yan, E. Tangdiongga, and A. M. J. Koonen, in *Proc. Performance Comparison of Multi-Wavelength Conversion using SOA-MZI and DSF for Optical Wavelength Multicast*, Athens, Greece, May 2007, pp. 1–10.
[25] B. Mikkelsen, S. L. Danielsen, C. Joergensen, R. J. S. Pedersen, H. N. Poulsen, and K. E. Stubkjaer, "All-optical noise reduction capability of interferometric wavelength converters," *IET Electron. Lett.*, vol. 32, no. 6, pp. 566–567, Mar. 1996.

N. Yan (S'02) received the B.Eng. degree in communication engineering from Zhongshan University, China, in June 2001, the M.Sc. degree (*Distinction*) in telecommunications from the University College London, U.K., in September 2003, and the Ph.D. degree from the Eindhoven University of Technology, Eindhoven, The Netherlands, in April 2008.

She was a Project Implementation Engineer at Siemens ICT, China, until September 2002. From January 2004, she was a Ph.D. researcher in the Electro-Optical Communication Systems Group, Eindhoven University of Technology. Since May 2008, she has been working in the Security and Technology Group, Advisory Business Unit, PricewaterhouseCoopers, The Netherlands.

J. del Val Puente received the M.Sc degree in telecommunications from the University of Valladolid, Spain, in July 2007. He carried out his M.S. thesis in the Electro-Optical Communications Group, Eindhoven University of Technology, Eindhoven, The Netherlands, from October 2006 to June 2007.

His research interests include optical communications, optical networks, and other new generations of telecommunications networks.

T. G. Silveira received the degree of "Licenciatura" in electronics and telecommunications engineering from the University of Aveiro, Portugal, in 2004, where he is currently pursuing the Ph.D. degree.

Between 2003 and 2004, he was with the Instituto de Telecomunicações, Aveiro, as a researcher. From 2004 to 2007, he was a researcher at Siemens/Nokia Siemens Networks. Currently, he is a System Engineer at Nokia Siemens Networks. His expertise areas are all-optical signal processing, nonlinear effects in semiconductor optical amplifiers, and optical transmission systems.

A. Teixeira (S'98–M'01) photograph and biography not available at the time of publication.

A. P. S. Ferreira (S'05) received the degree of "Licenciatura" in electronics and telecommunications engineering from the University of Aveiro, Portugal, in 2004, where she is currently pursuing the Ph.D. degree.

Since 2003, she has been with the Instituto de Telecomunicações, Aveiro, as a researcher. Her interest areas include optical transmission systems, advanced modulation formats, and RoF systems. She collaborates on several national and European projects.

E. Tangdiongga received the M.Sc. and Ph.D. degrees from the Eindhoven University of Technology (TU/e), Eindhoven, The Netherlands, in 1994 and 2001, respectively.

He is an Assistant Professor at the TU/e. In 1994, he joined the COBRA Research Institute. From 2001 to 2003, he participated in the EU FASHION project. Since January 2008, he has been working on optical signal transport and switching for short-haul communications in EU FP7 ICT research programs ALPHA (http://www.ict-alpha.eu), POF-PLUS (http://www.ict-pof-plus.eu), and Euro-Fos (http://www.euro-fos.eu). In 2005, he was on a sabbatical leave at Fujitsu Research Labs in Japan working on signal processing using highly nonlinear fibres and quantum-dot semiconductor optical amplifiers.

P. Monteiro (M'00) was born in Coimbra, Portugal, in 1964. He received the diploma and doctoral (Ph.D.) degrees in electronics and telecommunications from the University of Aveiro, Portugal, and the M.Sc. degree from the University of Wales, U.K.

He is a Research Manager at Nokia Siemens Networks Portugal and an Associate Professor at the University of Aveiro, where he has been teaching courses in telecommunications. He is also a researcher at the Instituto de Telecomunicações. His main research interests include high-speed optical communications for access and core networks, as well as fixed-mobile convergence. He has participated in several national and European projects and he is currently the project coordinator of the large-scale integrating project FUTON (FP7 ICT-2007–215533). He has authored/co-authored more than 15 patent applications and over 200 refereed papers and conference contributions.

Dr. Monteiro has acted as a reviewer for the IEEE/OSA JOURNAL OF LIGHTWAVE TECHNOLOGY; *IEE Electronics Letters*; *ETRI Journal*; *OSA Journal of Optical Networking* (JON); and *SPIE Optical Engineering*.

A. M. J. Koonen (M'00–SM'01–F'07) received the M.Sc. degree (*cum laude*) in electrical engineering from the Eindhoven University of Technology, Eindhoven, The Netherlands, in 1979.

He was with Bell Laboratories in Lucent Technologies as a Technical Manager of applied research for more than 20 years. He was a part-time Professor at the Twente University, Enschede, The Netherlands, from 1991 to 2000. Since 2001, he has been a Full Professor at the Eindhoven University of Technology in the Electro-optical Communication Systems Group at the COBRA Institute, where he has been the Chairman of this group since 2004. His current research interests include broadband fiber access and in-building networks, radio-over-fiber networks, and optical packet-switched networks. Currently, he is involved in a number of access/in-home projects in the Dutch Freeband program, the Dutch IOP Generieke Communicatie program, and the EC's FP7 ICT program.

Prof. Koonen has been a Bell Laboratories Fellow since 1998 and a member of the LEOS Board of Governors since 2007.